

A Temperature Error Correction Method for a Thermometer Screen

J. YANG* AND Q.Q. LIU

Jiangsu Key Laboratory of Meteorological Observation and Information Processing, Nanjing 210044, China
and

Jiangsu Collaborative Innovation Center on Atmospheric Environment and Equipment Technology,
Nanjing 210044, China

(Received 23 September, 2016)

Due to solar radiation exposure, air flowing inside a thermometer screen may produce a measurement error of 0.8°C or higher. To improve the air temperature observation accuracy, a temperature error correction method is proposed. The correction method is based on a computational fluid dynamics method and a genetic algorithm method. The computational fluid dynamics method is implemented to analyze and calculate the temperature errors of a screen under various environmental conditions. Then, a temperature error correction equation is obtained by fitting the computational fluid dynamics results using the genetic algorithm method. To verify the performance of the correction equation the screen and an aspirated temperature measurement platform are characterized in the same environment to conduct the intercomparison. The aspirated temperature measurement platform serves as an air temperature reference. The mean temperature error given by measurements is 0.77°C , and the mean temperature error given by correction equation is 0.79°C . This correction equation allows the temperature error to be reduced by approximately 97.5%.

DOI: [10.12693/APhysPolA.132.1301](https://doi.org/10.12693/APhysPolA.132.1301)

PACS/topics: temperature error, surface air temperature, computational fluid dynamics, screen

1. Introduction

Near surface air temperature is a basic information of climate change forecasting, data assimilation of satellite, weather forecasting, meteorological disaster warning. In recent years, a series of researches has been focused on the surface air temperature [1–6]. Haines et al. concluded that the air temperature increased 0.09°C by analyzing the data of satellite observation, and concluded that the air temperature increased 0.17°C by researching the data of weather stations [7]. Dillon et al. concluded that the air temperature increased 0.4°C and 0.95°C in tropical and northern hemisphere areas, respectively, by analyzing the data in the period 1961–2009, of 3186 weather stations throughout the world [8]. In conclusion, the magnitude of air temperature change is on the order of 0.1°C per decade. In order to observe the global, large scale, and local climate change accurately, to study the influence of aerosol and the solar radiation on the climate, and to research the change of content of water vapor, CO_2 , methane and other greenhouse gases quantitative, the measurement accuracy of the air temperature observation system should be on the order of or less than 0.01°C .

Because the temperature stability of the fixed points of water, gallium, indium and mercury can be within the order of $\pm 0.0002^{\circ}\text{C}$, and because the temperature measurement accuracy of a 1595A super-thermometer from Fluke is up to $\pm 0.000015^{\circ}\text{C}$, the accuracy of the platinum

temperature sensor probe may be able to reach $\pm 0.01^{\circ}\text{C}$ by utilizing the 1595A super-thermometer and the fixed points of International Temperature Scale of 1990 (ITS-90) [9]. Compared to the temperature error caused by solar radiation, the error induced by electronic devices and circuit is 12 orders of magnitude lower. To minimize the influence of solar radiation, a temperature sensor probe needs to be housed in a screen. Ideally, the screen can prevent the direct solar radiation, reflected solar radiation and surface upward longwave radiation from heating the probe, and can allow adequate airflow to ventilate the probe. Nevertheless, the reflectivities of the screen is incapable of reaching 100%, it may still generate radiation heating significantly, which causes the air into the internal being heated, and then produces temperature error. In addition, the structure of the screen is harmful to air circulation, which reduce the response rate of the inner probe [10, 11].

A number of studies have investigated the performance of screens. Erell et al. concluded that the mean temperature errors of the screens were up to 0.8°C by performing a series of comparative measurements [12]. The wind [13], radiation [14], and different coatings [15] displayed remarkable impacts on the energy balance of the screens, which might lead to $2\text{--}8^{\circ}\text{C}$ temperature errors under the adverse conditions that include weak wind of $\leq 1\text{ m/s}$ and high solar radiation intensity of $\geq 800\text{ W/m}^2$ [16–19]. Brock et al. concluded that the temperature error of a Gill radiation screen might be up to 8°C , when the wind speed was smaller than 0.2 m/s [20]. Lopardo et al. indicated a senescent screen might cause a large measurement error. Due to solar and weather exposure, the screens age and their coatings color changed from bright

*corresponding author; e-mail: yangjie396768@163.com

reflecting white to light beige. The temperature measured with the older screen was larger, and the maximum instantaneous difference was 1.63°C (for 0–5 years comparison) in daytime. Because the new screen also had temperature error, the temperature error of the older screen was larger than 1.63°C [21]. Generally, because the wind speeds are larger than 1 m/s , and because the screens are cleaned regularly, typical temperature errors of the screens range from $0.5\text{--}2.5^{\circ}\text{C}$ [22–27]. In conclusion, the screens may have difficulty to meet the present air temperature measurement accuracy requirements.

Because the flowing air can facilitate the diffusion of radiant heat, the temperature error can be reduced with the increase of wind speed through the screen. Hence, a high performance screen needs to be mechanically aspirated to increase the wind speed. For example, the range of wind speed of a 43502 aspirated screen manufactured by R.M. Young is 511 m/s . The temperature error induced by solar radiation is 0.2°C , when the wind speed and the solar radiation intensity are 11 m/s and 1000 W/m^2 , respectively. Thomas and Smoot proposed a new aspirated screen. The temperature error of the new aspirated screen was approximately 0.2°C , which hardly meets the demand of high accuracy observation [28]. An air pump driven by relatively high power seems to be necessary to achieve higher wind speed, if a temperature error of 0.1°C or even lower is desired. However, the power requirement and maintenance cost of such systems limits the applications of the aspirated screens. Most of the solar power supply system in weather stations cannot support the power demand, and the environmental factors such as dust, snow, insects, may compromise the long-term reliability of the fan. In conclusion, it is difficult for the aspirated screens to be widely applied by the weather stations in near future.

It has been pointed out by a World Meteorological Organization (WMO) report that investigations into the wind attenuation ratio modeling by using a computational fluid dynamics (CFD) method, and into estimation of the temperature error were both necessary [29]. CFD is a numerical simulation method that can model fluid flow and heat transfer in a multi-physical field [30, 31]. Richardson modeled the airflow through a Gill screen using a CFD software Fluent to attain the airflow profile inside the screen. The model was relatively simple, and the simulation results could offer only wind speed and direction inside the screen [32]. Because of the limited level of maturity, the CFD technologies in 1990s and early 2000s were unable to construct a heat transfer model of the screens. As a result, the numerical results of the temperature distribution and temperature error were unable to be obtained.

In this paper, a radiation error correction method is proposed. The correction method is based on a CFD method and a genetic algorithm (GA) method. GA is a heuristic algorithm, which is used to find optimal or near-optimal solutions for complex optimization problems. The CFD method is implemented to analyze and

calculate the radiation error of a screen under various environmental conditions. Then, a radiation error correction equation is obtained by fitting the CFD results using a GA method. The application of this radiation error correction method may potentially be used to correct historical air temperature data.

2. Radiation error correction method

2.1. Computational fluid dynamics model

A screen with a white coating is recommended by WMO to ensure a high surface reflection coefficient. In order to obtain the temperature errors of the screen, a CFD model is established. A platinum resistance temperature sensor probe is located on the axis of symmetry, midway between the top and bottom of the screen. A temperature measurement module that includes a high accuracy thermometer circuit is placed inside a protective case (Fig. 1).

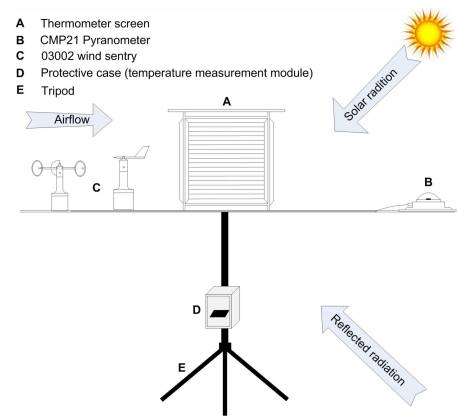


Fig. 1. Layout of the screen.

A grid software ICEM CFD is used to mesh the CFD model. The technology of unstructured mesh is adopted to generate a tetrahedral mesh. A CFD software Fluent is used to calculate the CFD model. A solar ray tracing model is used to load solar radiation. A standard $k\text{--}\varepsilon$ model, a SIMPLE algorithm and a standard initialization method are employed in the numerical computation. To solve the momentum, energy and turbulence parameters, a first order upwind method is applied in the CFD model. Boundary conditions of the CFD model are set according to the physical environment including the reflectivities of the surfaces of grassland and screen. The velocity inlet type and pressure outlet type are applied as boundary conditions for airflow inlet and airflow outlet, respectively. The density and thermal conductivity of the wooden thermometer screen are 700 kg/m^3 and 0.173 W/(m K) , respectively.

2.2. Modeling of temperature and velocity fields

In order to obtain the temperature error of the screen, the CFD model of the screen is analyzed in the identical environments. The wind speed and solar radiation

intensity are 2 m/s and 1000 W/m², respectively. The reflectivities of the surfaces of grassland and screen are 20% and 87%, respectively. The air velocity and temperature fields are shown in Fig. 2.

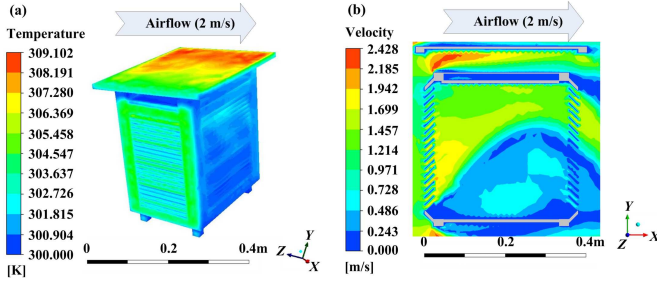


Fig. 2. Simulation results of the temperature and velocity fields: (a) the temperature field of the screen, (b) the velocity field.

The temperature error of the temperature sensor probe inside the screen is 0.288 °C (Fig. 2a). The wind speed at the center point of the screen is 0.313 m/s (Fig. 2b). It can be seen that the screen has difficulty to meet the present air temperature measurement accuracy requirements.

2.3. Correction of temperature error

The CFD method is applied to calculate the temperature errors of the screen at the conditions of various radiation intensities and wind speeds. The range of wind speed is 0.28 m/s, and the solar radiation intensity ranges from 100 to 1200 W/m². The CFD results are shown in Fig. 3.

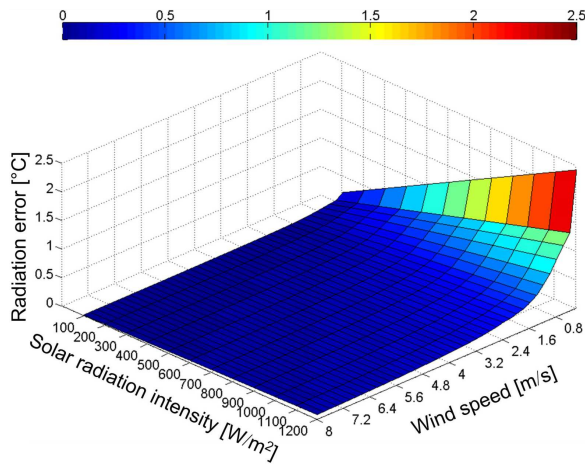


Fig. 3. Relationship among wind speed, solar radiation intensity, and temperature error.

The temperature error diminishes with increasing wind speed, and increases with increasing solar radiation intensity. The temperature error is 2.411 °C, when the solar radiation intensity and the wind speed are 1200 W/m² and 0.2 m/s, respectively. When the wind speed is smaller

than 1 m/s, the temperature error increases significantly with decreasing wind speed (Fig. 3).

Because the CFD method can only obtain limited temperature error results, a correction equation for temperature error may be needed. In order to obtain the correction equation, the GA method is applied to fit the CFD results.

$$\Delta T = \frac{p_1 + p_2 V + p_3 V^2 + p_4 V^3 + p_5 I + p_6 I^2}{1 + p_7 V + p_8 V^2 + p_9 I + p_{10} I^2}, \quad (1)$$

where $p_1 = -0.138$, $p_2 = 0.349$, $p_3 = 0.151$, $p_4 = 1.601 \times 10^{-2}$, $p_5 = 5.422 \times 10^{-3}$, $p_6 = 2.036$, $p_7 = 7.636$, $p_8 = 0.468$, $p_9 = 3.874 \times 10^{-4}$ and $p_{10} = -1.233$. V and I are wind speed and solar radiation intensity, respectively.

In order to verify the performance of the correction Eq. (1), a comparison between the CFD results and the results calculated by the correction Eq. (1) has been performed. Fifty CFD results shown in Fig. 3 are chosen randomly. The V and I in the correction Eq. (1) are substituted by the corresponding wind speeds and solar radiation intensities of the fifty CFD results, and then the fifty results calculated by the correction Eq. (1) are obtained. The maximum difference between the CFD results and correction results is smaller than 0.003 °C. In conclusion, the correction Eq. (1) may reflect the CFD results accurately. The temperature error can be predicted by substituting the measurement results of the wind speed and the solar radiation intensity into the correction Eq. (1), and then the air temperature observed results can be modified.

3. Experimental setup

The air temperature observation experiments in the field at Nanjing University of Information Science and Technology Site (32.12°N, 118.42°E, elevation 22 m) are implemented on clear days. The screen and an aspirated temperature measurement platform are mounted onto a frame at a height of 1.5 m over grass. A CMP21 Pyranometer manufactured by Kipp & Zonen is used to obtain the solar radiation intensity, and a 03002 wind sentry manufactured by R.M. Young Co. is adopted to measure the wind speed and direction. The ITS-90 fixed points and the 1595A super-thermometer are utilized to calibrate the temperature sensor probe. The instruments are shown in Fig. 4.

The aspirated temperature measurement platform consists of a platinum resistance temperature sensor probe, an L-shaped radiation shield, a stepping motor, and a centrifugal fan. The inner airflow velocity of the L-shaped shield is as large as 20 m/s. The L-shaped shield can horizontally rotate under the control of a software to minimize the error caused by the heated shield. The temperature error of the aspirated platform calculated using the CFD method is 0.002 °C, when the solar radiation intensity is 1000 W/m². Therefore, the measured value of the aspirated platform can be regarded as an accurate air temperature reference.



Fig. 4. Photos of the experimental setup: (a) the entire experimental field, (b) and (c) the screen and the aspirated temperature measurement platform, respectively.

4. Analysis on measured results and corrected results

In order to verify the actual performance of the correction Eq. (1), a number of comparisons have been performed. The corrected results can be obtained by substituting the measured values of the wind speeds and the solar radiation intensities into the correction Eq. (1). The temperature errors given by measurements and calculated radiation errors are shown in Fig. 5.

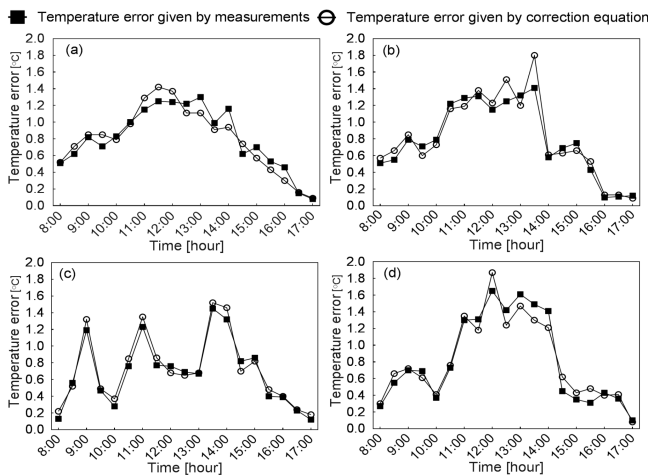


Fig. 5. The temperature errors given by measurements and the temperature errors given by correction Eq. (1) at different times: (a) 27 February 2016, (b) 29 February 2016, (c) 1 March 2016, (d) 14 March 2016.

During the daytime, the temperature errors are relatively large at noon, because the solar radiation intensity at this period of time is at the highest level in the day. The mean measured temperature error is 0.77°C , and the mean corrected temperature error is 0.79°C .

The accuracy of the correction Eq. (1) can be evaluated by using a root mean square error (RMSE), a mean absolute error (MAE), and an error reduction ratio r in Eqs. (2), (3), and (4), respectively

$$\text{RMSE} = \sqrt{\frac{\sum_{i=1}^n (E_{ce} - E_{me})^2}{n}}, \quad (2)$$

$$\text{MAE} = \frac{\sum_{i=1}^n |E_{ce} - E_{me}|}{n}, \quad (3)$$

$$r = \frac{E_{bc} - E_{ac}}{E_{bc}} \times 100\%, \quad (4)$$

where E_{me} is the measured temperature error, E_{ce} is the corrected temperature error, n is the total number of sampling, E_{bc} is the temperature error before correction, and E_{ac} is the temperature error after correction.

From Eqs. (2) and (3), the MAE and the RMSE between the corrected results and the measured results are 0.231°C and 0.327°C , respectively. It is clear that the difference between these results is a few orders of magnitudes smaller than the temperature errors of the screen. From Eq. (4), the correction Eq. (1) allows the temperature error to be reduced by approximately 97.5%. The accuracy of the correction method proposed in this research can be demonstrated.

5. Conclusions

In this paper, a temperature error correction method is proposed for obtaining high accuracy air temperature measurement results. Numerical modeling has been performed by using a CFD method under the conditions of various solar radiation intensities and wind speeds. A temperature error correction equation is obtained by fitting the CFD results employing a GA method. A screen and an aspirated temperature measurement platform are characterized in one site to conduct air temperature comparison experiments. The following conclusions may be obtained:

1. The temperature error increases with the solar radiation intensity, and decreases with the increase of wind speed.
2. The temperature error is reduced by approximately an order of magnitude by using the temperature error correction method proposed in this paper, which may be able to serve for climate change research and other fields.
3. The temperature error correction method can be used on a variety of screens.

Acknowledgments

This work was supported by the Special Scientific Research Fund of Meteorological Public Welfare Profession of China (GYHY200906037 GYHY201306079), the National Natural Science Foundation of China (41275042, 41605120) the Priority Academic Program Development of Jiangsu Higher Education Institutions (PAPD-II), and the Joint Fund of Jiangsu Key Laboratory of Meteorological Observation and Information Processing and Jiangsu Technology and Engineering Center of Meteorological Sensor Network (KDXS1504).

References

- [1] P.P. Harris, C. Huntingford, P.M. Cox, *Philos. Trans. R. Soc. B* **363**, 1753 (2008).
- [2] J.R. Toggweiler, R. Joellen, *Nature* **451**, 286 (2008).
- [3] R.A. Kerr, *Science* **334**, 173 (2011).
- [4] Z.A. Holden, J.T. Abatzoglou, C.H. Luce, L.S. Baggett, *Agric. For. Meteorol.* **151**, 1066 (2011).
- [5] J. Balanyá, J.M. Oller, R.B. Huey, G.W. Gilchrist, L. Serra, *Science* **313**, 1773 (2006).
- [6] A.P. Schurer, G.C. Hegerl, S.P. Obrochta, *Geophys. Res. Lett.* **42**, 5974 (2015).
- [7] A. Haines, A.J. McMichael, S. Kovats, M. Saunders, *BMJ Clin. Res.* **316**, 1530 (1998).
- [8] M.E. Dillon, W. George, R.B. Huey, *Nature* **467**, 704 (2010).
- [9] H. Preston-Thomas, *Metrologia* **27**, 3 (1990).
- [10] R.G. Harrison, C.R. Wood, *Q.J. Roy. Meteor. Soc.* **138**, 1114 (2012).
- [11] P.P. Harris, C. Huntingford, P.M. Cox, *Philos. Trans. R. Soc. B* **363**, 1753 (2008).
- [12] E. Erell, V. Leal, E. Maldonado, *Bound-Layer Meteorol.* **114**, 205 (2005).
- [13] X. Lin, K.G. Hubbard, G.E. Meyer, *J. Atmos. Oceanic Technol.* **18**, 329 (2010).
- [14] S.J. Richardson, F.V. Brock, S.R. Semmer, C. Jirak, *J. Atmos. Oceanic Technol.* **16**, 1862 (1999).
- [15] M. Fuchs, C.B. Tanner, *J. Appl. Meteorol.* **4**, 544 (1965).
- [16] S.P. Anderson, M.F. Baumgartner, *J. Atmos. Oceanic Technol.* **15**, 157 (1998).
- [17] K.G. Hubbard, X. Lin, E.A. Walter-Shea, *J. Atmos. Oceanic Technol.* **18**, 851 (2001).
- [18] M. Mauder, R.L. Desjardins, Z. Gao, R.V. Haarlem, *J. Atmos. Oceanic Technol.* **25**, 2145 (2008).
- [19] K.G. Hubbard, X. Lin, *Geophys. Res. Lett.* **29**, 67-1 (2002).
- [20] F.V. Brock, K.C. Crawford, R.L. Elliott, G.W. Cuperus, S.J. Stadler, H.L. Johnson, M.D. Eilts, *J. Atmos. Oceanic Technol.* **12**, 5 (1995).
- [21] G. Lopardo, F. Bertiglia, S. Curci, G. Roggero, A. Merlone, *Int. J. Climatol.* **34**, 1297 (2014).
- [22] C. Georges, G. Kaser, *J. Geophys. Res.* **107**, ACL 15-1 (2002).
- [23] R. Nakamura, L. Mahrt, *J. Atmos. Oceanic Technol.* **22**, 1046 (2005).
- [24] Z.A. Holden, A.E. Klene, R.F. Keefe, G.G. Moisen, *Agric. For. Meteorol.* **180**, 281 (2013).
- [25] R. Kurzeja, *Bound-Layer Meteorol.* **134**, 181 (2010).
- [26] L.B. MacHattie, *Ecology* **46**, 533 (1965).
- [27] M.C. Perry, M.J. Prior, D.E. Parker, *Int. J. Climatol.* **27**, 267 (2007).
- [28] C.K. Thomas, A.R. Smoot, *J. Atmos. Oceanic Technol.* **30**, 526 (2013).
- [29] A. Barnett, D.B. Hatton, D.W. Jones, *WMO Report No. 66* (1998).
- [30] A.T. Inan, T. Sisman, *Acta Phys. Pol. A* **127**, 1145 (2015).
- [31] B. Önen, Y. Yıldırım, E. Avcu, A. Çınar, *Acta Phys. Pol. A* **127**, 1225 (2015).
- [32] S.J. Richardson, *J. Atmos. Oceanic Technol.* **12**, 951 (1995).